Giant Magnetoresistance and Anomalous Hall Effect in Co-Ag and Fe-Cu, Ag, Au, Pt Granular Alloys

Gang Xiao, J. Q. Wang, and Peng Xiong
Department of Physics, Brown University, Providence, Rhode Island 02912, USA

Abstract–**Magnetotransport and magnetic properties have been studied in Co-Ag and Fe-Cu, Ag, Au, Pt alloys. In every system except Fe-Pt, giant magnetoresistance (GMR) was observed. We have characterised the GMR effect as we varied the volume fraction of the magnetic particles, as well as the particle size. We have also observed anomalous Hall effect and will present other transport parameters obtained in these systems.**

I. INTRODUCTION

The study of electron transport in artificial structures has become an important trend in condensed matter physics and materials science. Many exciting electron behaviors have been discovered in structural configurations different from the conventional homogeneous structures. Among the new behaviors, the giant magnetoresistance (GMR) effect is particularly astounding[1-3]. In an applied magnetic field, certain magnetic multilayers display a large response in resistance by as much as 100%. Recently, a stunning development has introduced a new dimension to the research of GMR. It has been reported that GMR also occurs in granular materials in which magnetic single-domain particles are embedded in a metallic matrix [4,5]. The mechanism of GMR is believed to be the spin-dependent scattering of the conduction electrons by magnetic entities[6,7]. At this primary stage, many important questions need to be addressed regarding GMR effect in granular structures. In this paper, we present a systematic study of magnetotransport, both resistivity and Hall effect, in five binary systems. Some universal features with respect to GMR have been uncovered. In addition, Hall effect is highly unconventional.

II. EXPERIMENT

All of our samples were made by using a high vacuum sputtering deposition system. Before each run, a background vacuum better than 1×10^{-7} Torr was first achieved. The Ar sputtering gas pressure was maintained at 4 mTorr. The silicon substrate used was kept at ambient temperature, except for Co-Ag system where the substrate was held at 77 K. The samples were either co-deposited from two individual pure targets or deposited with a single composite target. In the co-deposition mode, the composition of a sample was set by the sputtering rate of each source. This was an efficient process which yielded many samples with different compositions after each pump-down. The samples fabricated by both methods exhibited very similar transport and magnetic properties. The thickness of a sample is between 200 nm to 1 μm. We made sure that all samples were thick enough to have the bulk properties. To induce phase separation, we annealed some samples at various temperatures (T_A) in vacuum ($\leq 1 \times 10^{-7}$ Torr). The duration was about 10-15 minutes.

The standard photolithography and wet-etching technique were used to pattern our samples for resistivity and Hall effect measurement. The magnetic properties were measured by employing a SQUID magnetometer. Transmission-electron-microscope (TEM) was used to probe the microstructure. X-ray diffraction was also used to obtain structural and phase information.

III. STRUCTURES

GMR in granular solid was discovered in Co-Cu alloys which consisted of two immiscible elements[4,5]. Thermal annealing induces phase separation which is considered crucial to GMR. We have chosen five binary alloy systems whose equilibrium phase diagrams differ substantially. In Co-Ag, Fe-Ag, and Fe-Cu systems[8], the mutual solubilities of the two elements in each system are very small or practically zero in equilibrium. Furthermore, they do not form concentrated alloys or intermetallic compounds. The phase diagram of the Fe-Au system [8] is similar to those of the above three systems, except that Fe is partially soluble in Au ($x < 10\%$). Fe-Pt [8], on the other hand, does have many intermetallics, and serves as a good counterpart to other systems. Because of the granular structure, we use the parameter of volume fraction (x) to specify a sample. The value of x was determined using the bulk density of each element.

Manuscript received February 15, 1993.

Sputtering deposition tends to generate metastable, or even amorphous, alloys, because of the inherent high quenching rate. As-sputtered samples are in general rather homogeneous, or if phase separation occurs, the precipitates are very small in size (1-2 nm). These samples can be annealed at various high temperatures to induce phase separation. The grain size increases steadily with temperature and duration.

For the Co-Ag system, we studied a series of samples, all having the same Co volume fraction of 20%, but with different thermal annealing history. X-ray and TEM analysis attest to the formation of a granular structure with Co and Ag entities. The Co particle size, about 2 nm at T_A = 200 C, increases to about 13 nm at the maximum T_A of 605 C. The annealing time was about 10 min.

In as-sputtered samples, X-ray analysis of the Fe_xAu_{100-x} series indicated that metastable *fcc* alloys form up to $x = 60\%$. Similarly, Fe_xCu_{100-x} samples have metastable *fcc* structure up to $x = 50\%$. Thermal annealing of $Fe_{50}Cu_{50}$ caused distinctive phase separation above 325 C. The as-sputtered Fe-Ag samples also have *fcc*-like structures when $x < 50\%$, however, the structural assessment was less conclusive due to the overlapping spectral lines of Fe and Ag metals. We point out that it is difficult to detect phase separation in as-sputtered samples, particularly in the Fe-poor region of an alloy. If phase separation occurs, the Fe grains are very small (1-2 nm). Also the atomic number Z of Fe is much smaller than that of Au or Ag. TEM results on some of our as-sputtered samples indicate the existence of very fine grains ($\sim$ 2 nm). A clear indication of phase separation was observed in the measurement of magnetic succeptibility, which can be explained by the superparamagnetic mechanism. Data fitting with Curie-Weiss relation gave the average magnetic particle size of about 2 nm.

All of the Fe-Pt samples form *fcc* solid solutions as indicated in x-ray diffraction measurement. No granular structure is expected in this system.

IV. RESULTS AND DISCUSSION

Of the five binary systems studied, only the Fe-Pt alloys fail to exhibit any GMR effect. The variation of magnetoresistance (MR) between H = 0 and 8 T is of the order of 1 %. Nevertheless, all of the Fe-Pt samples including a sample with x = 8% are strongly ferromagnetic with enhanced Fe magnetic moment ($\sim 2\mu_{Fe}$ / Fe atom).

Co-Ag, Fe-Ag, Cu, Au systems display appreciable GMR effect at certain concentrations. They share the common feature that all are immiscible or nearly immiscible systems. This indicates that certain degree of magnetic heterogeneity is necessary for the appearance of GMR. In an heterogeneous system, the volume fraction of the active component is an important parameter. We have fabricated the above systems over a large volume fraction range. MR was measured in a magnetic field (H) range of -8 to 8 Tesla. Fig. 1 shows the MR, $\Delta\rho_{xx}/\rho_{xx}$ (referred to the zero field ρ_{xx}), obtained with H parallel and perpendicular to a film for some representative Fe_xAg_{100-x} samples. We limited our measurement to low temperature (T = 4.2K) because there is no complication from phonon and magnon excitations. The electron transport is mainly affected by disorder scattering as well as by spin-dependent magnetic scattering.

The magnitude of MR in Fig. 1 is rather large, particularly, when x is in the range of 13 to 24%. Another interesting feature is that MR is anisotropic, even though one would expect granular solids tend to be isotropic. The anisotropy in MR is in fact the consequence of the anisotropy in magnetisation (M) in different H orientation. Fig. 2 shows the magnetisation curves at T = 4.2 K

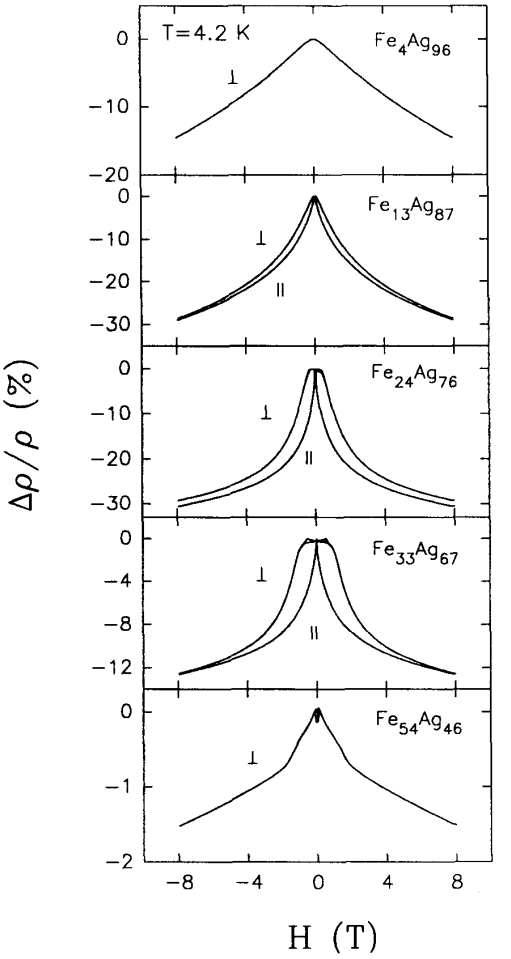

FIG. 1. Magnetoresistance vs. in-plane (||) and out-of-plane (⊥) magnetic field for five representative Fe_xAg_{100-x} samples at $T = 4.2$K.

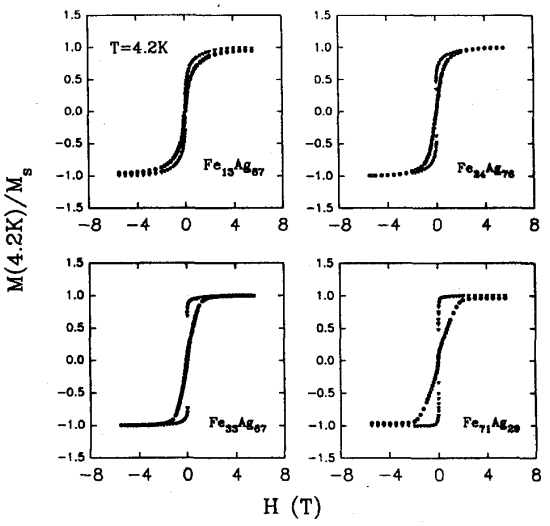

FIG. 2. Perpendicular and parallel magnetic hysteresis curves for four representative Fe_xAg_{100-x} samples at $T = 4.2$ K. The curves with lower saturation fields are obtained in a parallel field.

for four representative samples with H parallel and perpendicular to the sample plane. We found that all of the samples including Fe_4Ag_{96} are ferromagnetic at T = 4.2 K and the saturated magnetisation is equal to that of the bulk Fe within our error limit. The anisotropy in M is caused by the thin-film shape anisotropy and possibly by the shape anisotropy of the individual particles. In the parallel configuration, M can be saturated more easily.

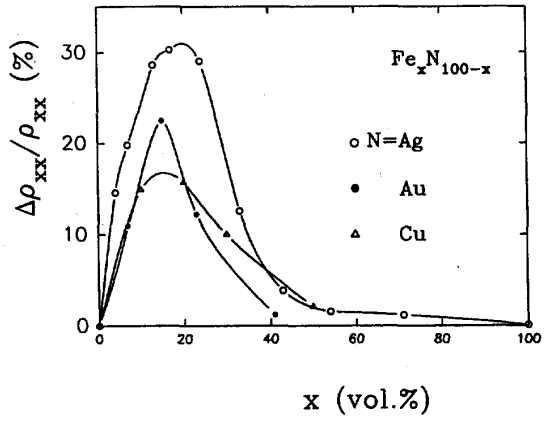

FIG. 3. The magnitude of GMR ($\Delta\rho_{xx}/\rho_{xx}$) vs. Fe volume fraction x for as-sputtered samples of Fe-Ag (open circles), Fe-Au (closed circles) and Fe-Cu (triangles). The lines are guides to the eyes. $T = 4.2$ K

Correspondingly, the initial slope in MR is steep. A large slope offers better sensitivity if a sample is to be used as a magnetic sensor.

For the Fe-Ag, Fe-Cu, and Fe-Au systems, the volume-fraction dependence of $\Delta\rho_{xx}/\rho_{xx}$ is shown in Fig. 3, where $\Delta\rho_{xx} = \rho_{xx}(0) - \rho_{xx}(8T)$. A universal behavior is uncovered. In each series maximum GMR effect is achieved at $x \approx 15-20\%$. On either side, GMR vanishes asymptotically towards x = 0 or x = 100%. This universal behavior is an important feature in magnetic granular solids with GMR. We feel that the suppression of GMR in the Fe-rich region is caused by the increasing probability of coalescence of the Fe clusters. As the cluster network becomes larger than the electron spin-flipping coherence length, GMR will decrease, for the same reason that in

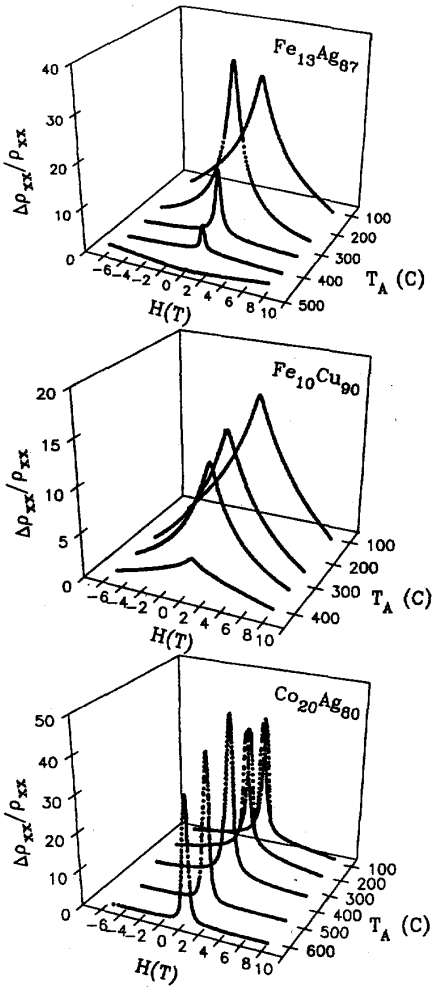

FIG. 4. Magnetoresistance vs. H at $T = 4.2$ K for $Fe_{13}Ag_{87}$, $Fe_{10}Cu_{90}$, and $Co_{20}Ag_{80}$ annealed at various temperatures T_A.

pure ferromagnetic metals MR is rather small.

Another crucial parameter in granular solids is the particle size, which may have strong influence on GMR. In Fig. 4, we show the MR of $Fe_{13}Ag_{87}$, $Fe_{10}Cu_{90}$, and $Co_{20}Ag_{80}$ annealed at increasing T_A. Again, a common behavior is revealed, in which GMR decreases as particle size becomes larger. Note that the quantity $\Delta\rho_{xx}/\rho_{xx}$ does not bear a monotonic relation with T_A. This is because the denominator ρ_{xx} contains contribution from disorder scattering which depends on T_A. On the other hand, $\Delta\rho_{xx}$, which depends on magnetic scattering only, does decrease monotonically with T_A. To assess the size effect more quantitatively, we have determined Co particle sizes in the $Co_{20}Ag_{80}$ samples using TEM and magnetic characterization. In Fig. 5, $\Delta\rho_{xx}$ is plotted against the inverse of the Co particle size, $1/r_{Co}$. A linear relation $\Delta\rho_{xx} \propto 1/r_{Co}$ is evidenced. $1/r_{Co}$ is in fact proportional to the surface-to-volume ratio of a particle. The linear relation suggests that interfacial magnetic scattering is responsible for the GMR. In Fig. 5, as we extrapolate the data to $1/r_{Co} = 0$ (i.e. in bulk Co, $r_{Co} \to \infty$), $\Delta\rho_{xx}$ is reduced substantially, but is not zero. This means that, at least in $Co_{20}Ag_{80}$, magnetic scattering inside the bulk of a particle cannot be completely ignored.

In addition to the evolution of the magnitude of GMR, another salient feature in Fig. 4 is the saturation process of MR. For the as-sputtered samples, MR remains unsaturated at the highest H. However, saturation becomes easier for samples annealed at higher T_A. This is yet another important feature of granular systems with GMR.

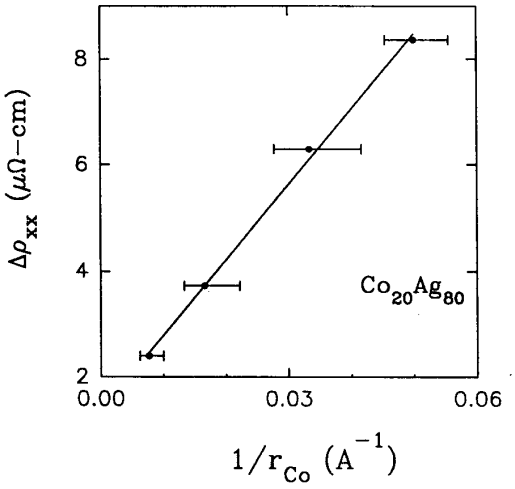

FIG. 5. $\Delta\rho_{xx} = \rho_{xx}(0) - \rho_{xx}(8T)$ at $T = 4.2$ K vs. the inverse of the Co particle size, $1/r_{Co}$, in $Co_{20}Ag_{80}$.

In application, one desires not only a large magnitude of GMR but also a fast saturation of MR in H. According to Fig. 4 both are not achieved concurrently, some compromise needs to be made.

To better characterize the spin-dependent scattering, we have also studied the Hall effect in our systems. Hall effect is also sensitive to the magnetic state of a material. It further provides crucial information on the carrier type, concentration, and electron mean free path if the resistivity is also known. Simultaneous study of Hall effect should be beneficial to a comprehensive understanding of GMR. Fig. 6(a) shows the Hall resistivity, ρ_{xy}, as a function of H at T = 4.2 K for $Co_{20}Ag_{80}$ samples annealed at various temperatures. The results can be treated phenomenologically as the sum of two components

$$\rho_{xy} = R_0[H + 4\pi M(1 - D)] + R_s 4\pi M, \qquad (1)$$

where the first term is due to the ordinary Hall effect (OHE) (D is the demagnetisation factor), and the second term, resulting from a magnetic scattering, is the extraordinary Hall effect (EHE) proportional to M [9]. We denote $\rho_{xy}^M = R_s 4\pi M$. R_s is negative in our samples. The most interesting feature in Fig. 6 is that the EHE component, ρ_{xy}^M, decreases rapidly at high annealing temperatures. The magnitude of EHE is measured by $\rho_{xy}^{M_s}$, which is obtained by extrapolating $\rho_{xy}(H)$ from the linear portion at high H to $H = 0$. In $Co_{20}Ag_{80}$ annealed samples, the saturated magnetization, M_s, is 142.9 emu/g within an error of $\pm$ 5% at T = 4.2 K. Therefore, $\rho_{xy}^{M_s} = CR_s$, where C is a constant.

EHE is caused by spin-orbit interaction between conduction electrons and disorders. Spin-orbit interaction [9] results in two distinctive mechanisms affecting the Hall effect. The first is the skew scattering which causes the electron trajectory to deflect asymmetrically from its original path [9]. The second mechanism, a quantum me-

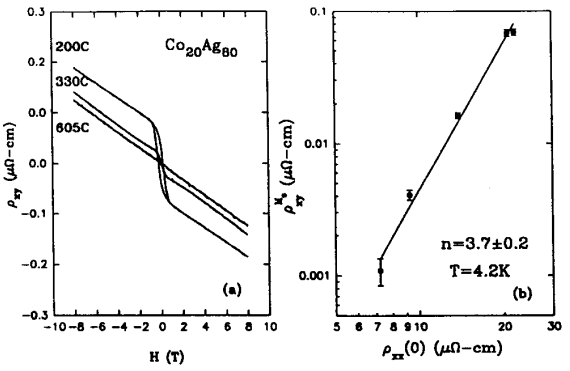

FIG. 6. (a) Hall resistivity $\rho_{xy}(H)$ at $T = 4.2$ K for $Co_{20}Ag_{80}$ samples annealed at 200, 330, and 605 C. (b) Correlation between $\rho_{xy}^{M_s}$ and ρ_{xx} for $Co_{20}Ag_{80}$. n is the exponent in $\rho_{xy}^{M_s} \propto \rho_{xx}^n$.

chanical effect, is the so-called side jump, in which the electron trajectory is displaced transversely by a distance Δy ($\approx 0.1 - 1\AA$) while the direction remains intact [9]. For skew scattering,

$$\rho_{xy}^{M_s} \propto \rho_{xx}. \quad (2)$$

For side jump,

$$\rho_{xy}^{M_s} \propto \rho_{xx}^2. \quad (3)$$

We plot $\rho_{xy}^{M_s}$ vs. ρ_{xx} in log scale in Fig. 6(b). The linear line obtained indicates that the correlation between the two quantities is still a power law, i.e. $\rho_{xy}^{M_s} \propto \rho_{xx}^n$. However the exponent n = 3.7 is the largest exponent ever observed. There is no mechanism that predicts such a large exponent [9].

In Fig. 6(b), the scaling relation is obtained using the ρ_{xx} value at H=0. We choose this value because it includes contributions from both disorder and magnetic scattering. It is arguable whether the extrapolated value from high field is more appropriate. However, using the extrapolated ρ_{xx} value does not alter the overall anomalous relation between $\rho_{xy}^{M_s}$ and ρ_{xx}. It leads to a deviation from the simple linear relation shown in Fig. 6(b). But a least square fit still yields an exponent of 3.7.

We feel that the large exponent, n, is still caused by the side-jump mechanism. However, unlike the conventional side-jump scattering where the scatterer is atomic in size, the scatterer in granular structure is much larger. The side-jump mechanism should be sensitive to the size of the scatterer. The anomalous GMR and EHE effects presented here call for a more unified approach in treating the magnetotransport of heterogeneous magnetic systems.

From the OHE at high H, we have calculated the carrier concentration, n_H, assuming the existence of a simple parabolic energy band. Independent of annealing temperature, n_H turns out to be 4.1×10^{22} cm^{-3}. Using Drude expression for resistivity, we have estimated the effective electron mean free path, λ_{eff}, at T = 4.2 K and H = 0. As expected, λ_{eff} increases from about 5 nm for the as-sputtered sample to 15 nm for a well-annealed sample. These numbers are rather close to the average Co particle sizes and the interparticle separations (when x = 20%), indicating that the dominant disorders are those caused by the grain boundaries.

For the Fe_xAg_{100-x} series, we have compiled some of the important electron transport parameters in Fig. 7 as functions of the Fe volume fraction. In order to separate the magnetic scattering from the disorder scattering, we present $\rho_{xx}(0)$ at H = 0 and $\Delta\rho_{xx}$ in Fig. 7 (a) and (b). $\Delta\rho_{xx}$ is solely due to the spin-dependent magnetic scattering. It is a better parameter to characterize GMR than the often used $\Delta\rho/\rho$, which includes contribution from disorder scattering (in ρ). In Fe_xAg_{100-x}, $\rho_{xx}(0)$ increases sharply with the addition of Fe, but it starts to saturate when x exceeds 10%.

In Fig. 7 (c), we show the effective carrier concentration, n_H, which is calculated from the OHE and is an estimate of the average n_H in granular solids. Using the

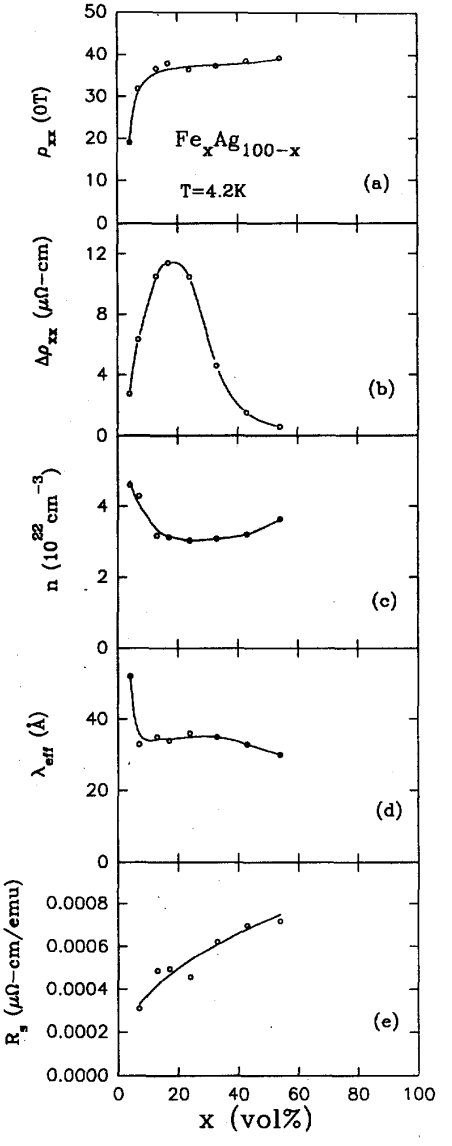

FIG. 7. Various determined transport parameters at T = 4.2 K for the Fe_xAg_{100-x} as-sputtered samples. (a) zero-field resistivity, $\rho_{xx}(0T)$, (b) change of resistivity between H = 0 and 8 T, $\Delta\rho_{xx}$, (c) Hall carrier concentration, n_H, (d) effective electron mean free path, λ_{eff}, (e) coefficient of the extraordinary Hall effect, R_s.

results of resistivity and Hall effect, we have also calculated the effective electron mean free path, λ_{eff}, as shown in Fig. 7 (d). One observes that λ_{eff} is short $(30-50\AA)$, and does not vary appreciably across the volume fraction range. Because of the dominance of grain boundary scattering, the cluster size should be around this length scale. Fig. 7 (e) shows R_s, which is the coefficient of EHE. The reason we use R_s rather than $\rho_{xy}^{M_s}$ $(\propto R_s M_s)$ is because M_s (per unit volume) is not a constant as the Fe content changes across x.

In summary, granular alloys involving magnetic transition elements (Fe, Co) and normal metal elements (Cu, Ag, Au) exhibit appreciable GMR effect. A common feature among these system is that a maximum GMR is achieved when the volume fraction of the magnetic particles is close to 15 - 20%. Thermal annealing, which abates disorder scattering and enlarges particle size, tends to suppress the GMR effect and to reduce the saturation magnetic field for MR. There is evidence showing the dominance of interfacial magnetic scattering in GMR. The Hall effect of these systems is also anomalous. The scaling relation between EHE and resistivity is highly unconventional in the $Co_{20}Ag_{80}$ system.

ACKNOWLEDGMENTS

We wish to thank C. L. Chien for useful discussion and for providing the Co-Ag samples for this study. This work was supported by National Science Foundation (NSF) Grant No. DMR-9121747. One of the authors (G.X.) wishes to thank the A.P. Sloan Foundation for a fellowship and NSF for the NSF Young Investigator Award.

REFERENCES

[1] M. N. Baibich, J. M. Broto, A. Fert, F. Nguyen van Dau, F. Petroff, P. Etienne, G. Creuset, A. Friederich, and J. Chaseles, "Giant magnetoresistance of (001)Fe/(001)Cr magnetic superlattices," Phys. Rev. Lett., vol. 61, pp. 2472-2475, November 1988.

[2] S. S. P. Parkin, R. Bhadra, and K. P. Roche, "Oscillatory magnetic exchange coupling through thin copper layers," Phys. Rev. Lett., vol. 66, pp. 2152-2155, April 1991.

[3] W. P. Pratt, Jr., S.-F. Lee, J. M. Slaughter, R. Loloee, P. A. Schroeder, and J. Bass, "Perpendicular giant magnetoresistances of Ag/Co multilayers," Phys. Rev. Lett., vol. 66, pp 3060-3063, June 1991.

[4] A. E. Berkowits, J. R. Mitchell, M. J. Carey, A. P. Young, S. Zhang, F. E. Spada, F. T. Parker, A. Hutten, and G. Thomas, "Giant magnetoresistance in heterogeneous Cu-Co alloys," Phys. Rev. Lett., vol. 68, pp. 3745-3748, June 1992.

[5] J. Q. Xiao, J. S. Jiang, and C. L. Chien, "Giant magnetoresistance in nonmultilayer magnetic systems," Phys. Rev. Lett., vol. 68, pp. 3749-3752, June 1992.

[6] R. E. Camley and J. Barnas, "Theory of giant magnetoresistance effects in magnetic layered structures with antiferromagnetic coupling," Phys. Rev. Lett. vol. 63, pp. 664-667, August, 1989.

[7] S. Zhang, P. M. Levy, and A. Fert, "Conductivity and magnetoresistance of magnetic multilayered structures," Phys. Rev. B, vol. 45, pp. 8689-8702, April 1992.

[8] *Iron-Binary Phase Diagrams* O. Kubaschewski, ed. Berlin: Springer-Verlag, 1982.

[9] L. Berger and G. Bergmann, "The Hall effect of ferromagnets," in *The Hall Effect and Its Applications*, C. L. Chien and C. R. Westgate, Eds. New York: Plenum, 1979, pp. 55-76.